UC San Diego

UC San Diego Previously Published Works

Title

Atomimetic Mechanical Structures with Nonlinear Topological Domain Evolution Kinetics

Permalink

https://escholarship.org/uc/item/81g7d89v

Journal

Advanced Materials, 29(19)

ISSN

0935-9648

Authors

Frazier, Michael J

Kochmann, Dennis M

Publication Date

2017-05-01

DOI

10.1002/adma.201605800

Copyright Information

This work is made available under the terms of a Creative Commons Attribution License, availalbe at https://creativecommons.org/licenses/by/4.0/

Peer reviewed

eScholarship.org Powered by the California Digital Library
University of California

Atomimetic Mechanical Structures with Nonlinear Topological Domain Evolution Kinetics

Michael J. Frazier and Dennis M. Kochmann*
Graduate Aerospace Laboratories, California Institute of Technology, Pasadena, California 91125, USA

Multi-welled energy landscapes are key to microstructural pattern formation observed in solids that undergo, e.g., phase transformations [1], ferroelectric/magnetic domain switching [2, 3], diffusive phase separation [4, 5], or deformation twinning [6]. The nonconvex energy entails a thermodynamic preference for what in mathematics is known as minimizing sequences [7]: assisted by applied fields and microstructural defects, homogeneous states of deformation (or of electro-magnetic fields) give way to energy-minimizing mixtures of domains (i.e., uniform regions in local energy minima) separated by a network of domain walls. Under load, domain walls move – a dissipative process that produces the macroscopically-observed hysteresis and is of importance for, e.g., shape memory alloys [8], ferroelectric poling [9], and multiferroics [10]. Here, we present a purely mechanical, size-independent structure (or metamaterial) that exhibits similar domain evolution phenomena, and we demonstrate via numerical examples that the system additionally obeys quantitatively analogous fundamental governing laws but with extreme tunability and experimental accessibility. This constitutes a new theoretical paradigm to capitalize on microstructural dynamic processes and to export the nonlinear kinetics to the structural scale, which admits experimental implementation.

The ever decreasing resolution in additive manufacturing techniques has created opportunities for the bottom-up design of novel (meta)materials. Examples include truss lattices and hierarchical nanotrusses with superior stiffness and strength scaling [11], auxetic behavior [12], thermal management [13], acoustic or phononic wave control [14, 15], and energy absorption [16]. Nature has inspired the emulation of atomic-scale architectures at the macroscopic, structural level, resulting in, e.g., acoustic metamaterials [17], topological defects and soft modes [18], and structural transitions [19]. At this level, topological transformations and domain patterning occur as a consequence of structural instability and the associated nonconvex energy landscape implying more than one stable equilibrium configuration. Despite various examples that realized static domain formation through patterning [18, 20, 21], no attempt has been made at exploiting their nonlinear dynamic evolution, although the controllable nonlinear hysteresis appears promising for applications from morphing surfaces and haptics to soft robotics and structural logic. Our goal is to show, by rigorous analysis and comparison between the new structure and microstructural processes, that microstructural kinetic domain evolution can be emulated by multistable mechanical metamaterials, which may inspire experimental realizations in the future.

Our mechanical analog translates the atomic-scale polarization found, e.g., in ferroelectrics, into a scalar polarization field that possesses one or two stable equilibria depending on the ambient conditions, just as the Landau-Devonshire energy density changes with temperature through a second-order phase transition [22–24]. This is likely the simplest and most instructive system possible to reproduce key features of atomic-scale structural transitions, viz. domain formation and switching (see Figure 1a and c). As shown in Figure 1e, we consider a 2D periodic array of elastically-connected bistable elements which drive the system towards domains of uniform polarization, while the elastic connections penalize and thus localize domain walls to interpolate between opposing phases. Our recent experiments [25, 26] showed that 1D arrays following the same blueprint give rise to stable transition waves that snap between the two stable states (Figure 1b) while propagating at constant speed, provided the bistable energy potential is non-symmetric, so that each snap releases elastic energy that propels the domain wall. Unlike topological zero-energy modes [18], these systems are statically determinate and the transition wave results from the stabilized competition between elastic energy release and dissipation through mechanical damping [27, 28].

We consider a 2D periodic network of cylindrical masses M with a single (rotational) degree of freedom φ, the *polarization*. A salient feature of the structure, multistability arises from elastic springs that attach eccentrically to each cylinder at one end and to an anchor point (elevated by a distance f_z) at the other (Figure 1f). The action of gravity on additional masses m eccentrically placed on the cylinders creates a torque when the rotation axis and gravity field are not aligned. The resulting multi-welled energy landscape can be tuned by (*i*) moving the elevated plane (i.e., a ceiling) of anchor points (by a distance f_x) and/or (*ii*) tilting the entire system (by angles α,β). In the level condition (i.e., $\alpha = \beta = 0$), choosing $f_x \neq 0$ imbues each element with multiple stable states $\varphi_i \neq 0$, limited to two by the addition of a torsional spring (relaxed at $\varphi = 0$). Moving ceiling and cylinders relative to each other so that $f_x \to 0$ turns the bistable energy (with *polar* stable configurations $\varphi_i \neq 0$) into a single energy well with stable *unpolar* ground state $\varphi = 0$.

The Hamiltonian of a 2D network with N periodically

* Corresponding author; email: kochmann@caltech.edu

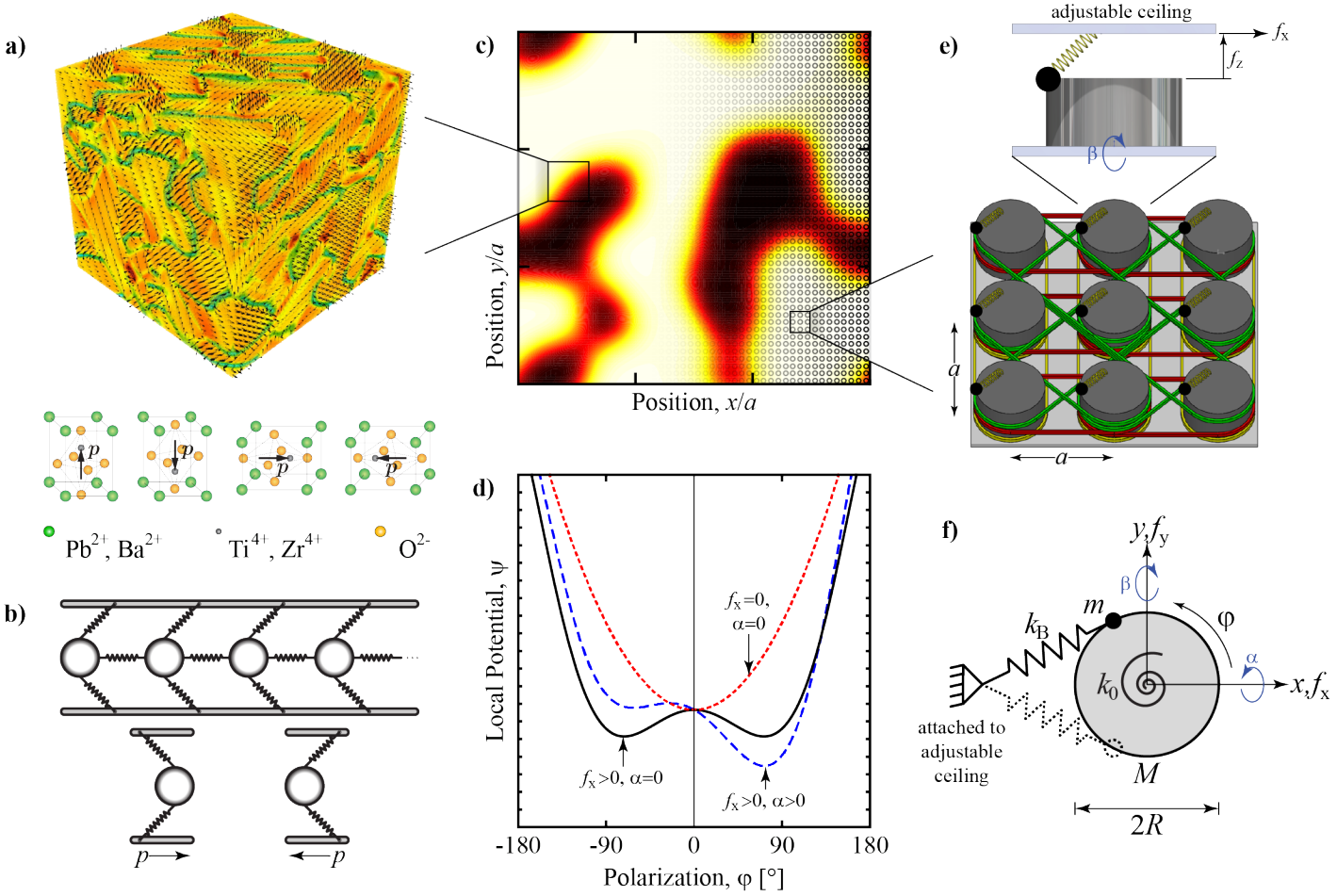

Figure 1. Phase transformations, ferroic domain switching, and diffusive phase separation are material processess enabled by a multi-welled energy landscape. a) Below the Curie temperature, ferroelectrics exhibit a spontaneous polarization due to broken crystal symmetry which displaces the central ion outside the midplane, creating a dipole. b) A mechanical system, e.g., in a 1D chain of bistable elements, may display a scalar polarization. c) The underlying kinetics of structural transformations are observed in discrete like continuous systems. d) Common to all, these systems possess a multi-welled energy landscape. e) Each element of our 2D mechanical system exhibits a bistable potential and, through the use of masses and springs (see schematic in f)), recovers all the processes mentioned previously. Tilting the mechanical structure by α and/or β (positive counter-clockwise when looking down the respective axis) permits a gravitational field to induce domain switching.

arranged cylinders of radius R is given by

$$\mathcal{H} = \sum_{i=1}^{N} \left[\frac{1}{2} I \dot{\varphi}_i^2 + \psi(\varphi_i, \boldsymbol{\theta}, \boldsymbol{f}) \right] + \sum_{i,j=1}^{N} V\left(\varphi_i - \varphi_j\right) \quad (1)$$

with I the total rotational inertia and $\psi(\varphi, \boldsymbol{\theta}, \boldsymbol{f})$ the nonlinear multi-welled energy resulting from springs and tunable via $\boldsymbol{\theta} = \{\alpha, \beta\}$ and $\boldsymbol{f} = \{f_\mathrm{x}, f_\mathrm{y}, f_\mathrm{z}\}$ [29]. If elastic bands link the cylinders (Figure 1e), then $V(\Delta\varphi) = k_{ij}(R\,\Delta\varphi)^2$ is an elastic interaction potential. In every realistic system, dissipation of kinetic energy through, e.g., friction is inevitable, thus motivating the inclusion of velocity-proportional damping with damping constant η in the governing equation of momentum balance (Hamilton's equation of motion). Hence, our discrete mechanical network is described by (for $i = 1, \ldots, N$, and writing $\psi' = \partial\psi/\partial\varphi$)

$$I\ddot{\varphi}_i + \eta\dot{\varphi}_i + \psi'(\varphi_i, \boldsymbol{\theta}, \boldsymbol{f}) - R^2 \sum_j k_{ij}\left(\varphi_i - \varphi_j\right) = 0. \quad (2)$$

Similar to viewing an atomistic ensemble from a perspective at greater scale, we now zoom out and observe the dynamic processes in a homogenized sense. Mathematically, this calls for taking the continuum limit as the inter-mass spacing a goes to zero. The resulting continuum model [29] based on a continuous rotational field $\varphi(\boldsymbol{x})$ is analogous to the polarization field in phase field models of domain evolution in, e.g., phase transformations, twinning, reaction-diffusion processes, and ferroelectrics [3, 4, 30–32]. Specifically, Equation (2) becomes

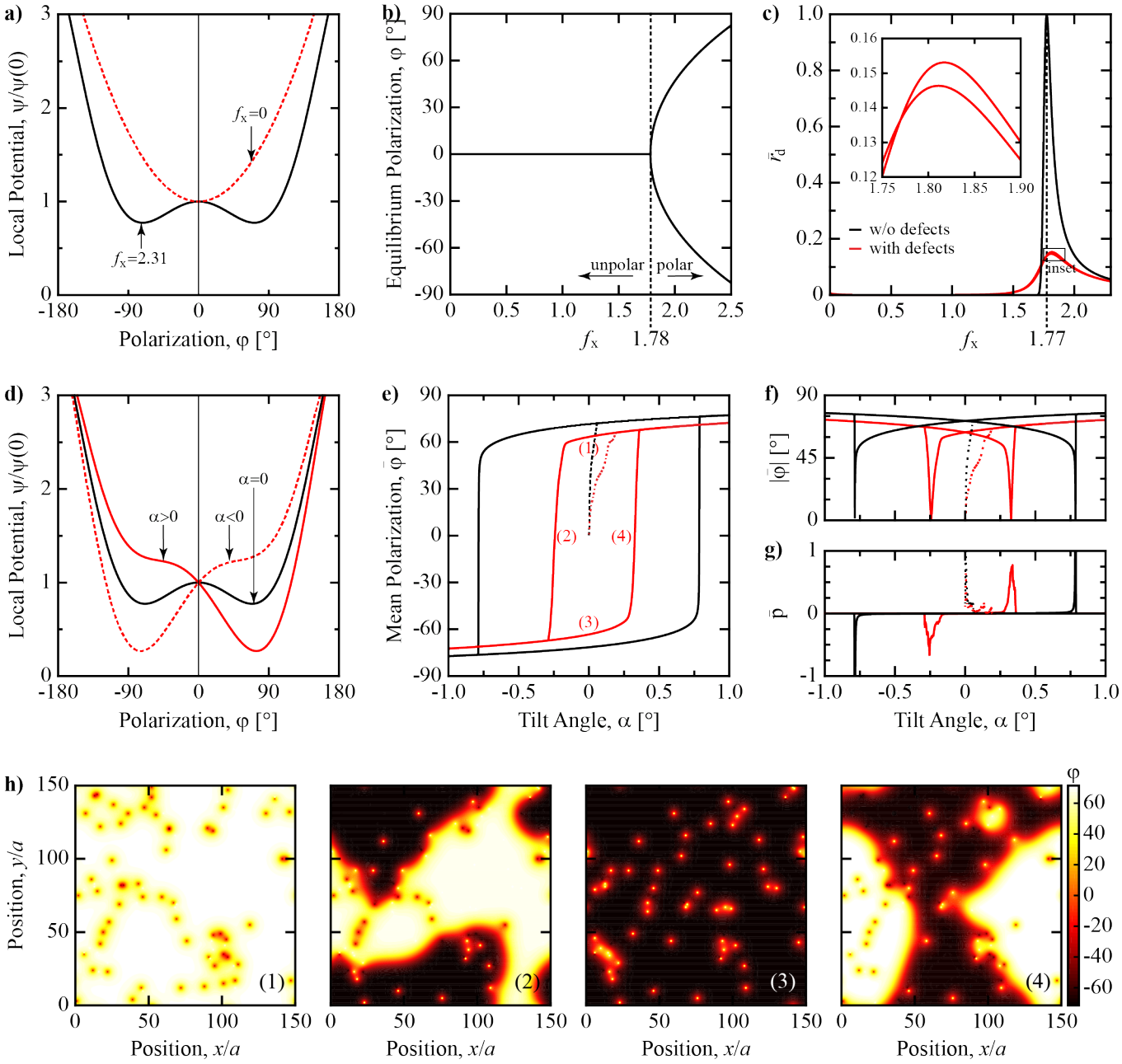

Figure 2. Phase transformations are induced externally through motion of the ceiling. a) The energy landscape becomes single-welled b) as the equilibrium polarizations coalesce in a smooth, second-order transformation. c) A peak in the total energy dissipation rate $\bar{r}_d$ (normalized to unity) reveals the transformation f_x in a system with (red) and without (black) defects. d) Tilting the structure by α applies a gravitational field biasing the energy landscape toward one polarization, leading to switching and characteristic hysteresis: mean e) polarization $\bar{\varphi}$, f) strain $|\bar{\varphi}|$, and g) momentum $\bar{p}$ (normalized by $p = 0.0135$). h) Defects act as nucleation sites, encouraging premature switching as depicted in system snapshots at qualitatively unique stages in the hysteresis.

[29]

$$\rho\ddot{\varphi} + \nu\dot{\varphi} = \frac{\partial}{\partial x_i}\left(\kappa_{ij}\frac{\partial\varphi}{\partial x_j}\right) - \psi'(\varphi, \boldsymbol{\theta}, \boldsymbol{f}) \qquad (3)$$

with the symmetric coefficients κ_{ij} determined by the periodic arrangement and connecting stiffnesses (thus allowing for system tunability to display different anisotropic domain wall energies), inertial density ρ and inverse mobility ν. Notice that, if there is isotropy ($\kappa_{ij} = \kappa\boldsymbol{I}$) and significant damping ($|\rho\ddot{\varphi}| \ll |\nu\dot{\varphi}|$) as in our recent 1D experiments [26], then we recover the well-known Allen-Cahn equation [33, 34] of phase separation,

i.e.,

$$\nu\dot{\varphi} = \kappa\,\Delta\varphi - \psi'(\varphi, \boldsymbol{\theta}, \boldsymbol{f}). \tag{4}$$

In our network, the elastic connections play the role of interfacial energy, while the on-site potential ψ mimics the multi-welled Landau-Devonshire energy [22–24], and frictional damping determines the mobility.

Below the Curie temperature T_c [2] asymmetry in the crystal structure leads to a polarized state in ferroic ceramics. Above this critical temperature, a phase transformation occurs resulting in an unpolar, centrosymmetric crystal structure. From an energy perspective, the $2d$ stable equilibria of the local potential (modeled, e.g., by Landau-Devonshire theory [22–24] in d dimensions) merge into a single minimum. As depicted in Figure 2a, our mechanical structure demonstrates the same transformation when moving the ceiling, viz., $f_\mathrm{x} \to 0$; two polarizations coalesce below a transformation "temperature" of $f_\mathrm{x} = 1.78$ (Figure 2b). Conveniently, knowledge of the functional form of ψ permits the transformation f_x to be predicted numerically [29]. A polynomial expansion of the on-site potential ψ can be used to approximate $\varphi_{1,2} = \varphi_{1,2}(f_x)$ in the polarized state, showing that the critical exponent of $1/2$ agrees with classical Ginzburg-Landau theory for ferroelectrics in 1D where the polarization scales with temperature $T \leq T_\mathrm{c}$ as $(T - T_\mathrm{c})^{1/2}$; see [29].

For materials, Differential Scanning Calorimetry (DSC) reveals the transformation temperature as a marked change in the heat flux required to control the sample temperature [35]. By analogy, in Figure 2c we observe a stark increase (peaking at $f_\mathrm{x} = 1.77$) in the total dissipation rate ("heat flux") $\bar{r}_\mathrm{d} = \sum_{i=1}^{N} \eta|\dot{\varphi}_i|^2$ when cycling f_x ("temperature") between polar and unpolar values (all numerical data are normalized [29]).

Like at the material level, the unrealistic absence of defects promotes a homogeneous transformation. Figure 2c shows lattice defects (a random subpopulation of cylinders [36] fixed in their initial polarization mimicking immobile dipoles, solutes, or vacancies [37]) offer nucleation sites during polarization and represent obstacles to depolarization. This leads to a direction-dependent shift in the transformation f_x.

In the polar phase, applying electric fields to pervoskite ceramics results in domain switching, a process which – through nucleation and domain wall motion – gradually compels the solid towards one polarization. The applied field biases the multi-welled energy through a linear tilt, propelling the domain switching. By analogy, tilting the system of oscillators about the x- and/or y-axis (Figure 2d) activates the gravitational component of the on-site potential. Sufficient rotation about the x-axis transforms the local potential to a single well energetically favorable to one polarization. Consequently, ferroic-like switching of the polarization is observed in response to gravitation. Classic hysteretic behavior is displayed when cycling the tilt angle beyond the critical values $\alpha = \pm\alpha_\mathrm{c}$ (with α akin to the coercive electric field) at which sudden, large changes in polarization occur.

Starting from a random initial distribution of φ, we induce domain switching by cyclically adjusting α ($\beta = 0$) in a gradual manner so as to minimize rate effects. Figure 2e shows a characteristic hysteresis loop, where tilt angle and mean rotation of the cylinders, respectively, are the system equivalent of, e.g., electric field and polarization for ferroelectrics. Following an initial transient period during which the noisy distribution of φ proceeds towards a homogeneous polarization, without nucleation sites, the system responds uniformly as the loop is traversed, experiencing a reversal of polarization at the critical tilt angles $\alpha_\mathrm{c} = \pm 0.76°$ predicted by ψ. Realistically, defects exist within the system, acting as a catalyst for switching by providing nucleation sites for the opposing polarization, reducing α_c. Thus, the loop is noticeably compressed in comparison to the defect-free scenario. Pinning of domain walls at defects is also apparent as in ferroelectrics [37, 38]. Figures 2f and 2g, respectively, depict the corresponding polarization and momentum loops, analogous to the strain (butterfly loop) and electric current hysteresis in ferroelectrics. The series of snapshots in Figure 2h (and Movie S1) illustrate the system throughout the hysteresis. Scenes (1) and (3), respectively, show a system of polarization φ_+ and φ_- with defects of opposing polarization clearly visible. Note that the scalar polarization field chosen here cannot differentiate between 180°- and 90°-domain walls; however, this objective is feasible through an extension (e.g., replacing rotations by translational motion).

For planar wave fronts, the balance between the energy release $\Delta\psi$ during the transition and the viscous drag (characterized by η) determines the energy density E_d and speed v of the domain wall resulting from Equation (2), which admits the theoretical scaling prediction [29]

$$E_\mathrm{d}/v \simeq \Delta\psi/2\eta. \tag{5}$$

As expected, wall motion occurs in the direction of descending energy (i.e., v and $\Delta\psi$ must be of the same sign [28]). Equation (5) is verified in Figure 3a for transitions propagating along different directions and within different elastic networks, showing convincing agreement for sufficiently wide [39] wave fronts. The width is widened (narrowed) by increasing (decreasing) the elastic band stiffness in the propagation direction. Similar effects are obtained if the lattice constants are of unequal magnitude. Discreteness effects manifest, e.g., for the isotropic case, through the slow convergence with increasing width w under 45° in contrast to 0° and 90° wave fronts; orientations of 45° encounter the sparsest packing of masses.

Differences between the mechanical metamaterial, governed by Equation (2), and the mesoscale phase field description of Equation (4) stem primarily from (*i*) discreteness effects and (*ii*) inertial effects. The former decay with increasing coupling k_{ij} between cylinders; the latter with increasing viscosity η and/or decreasing iner-

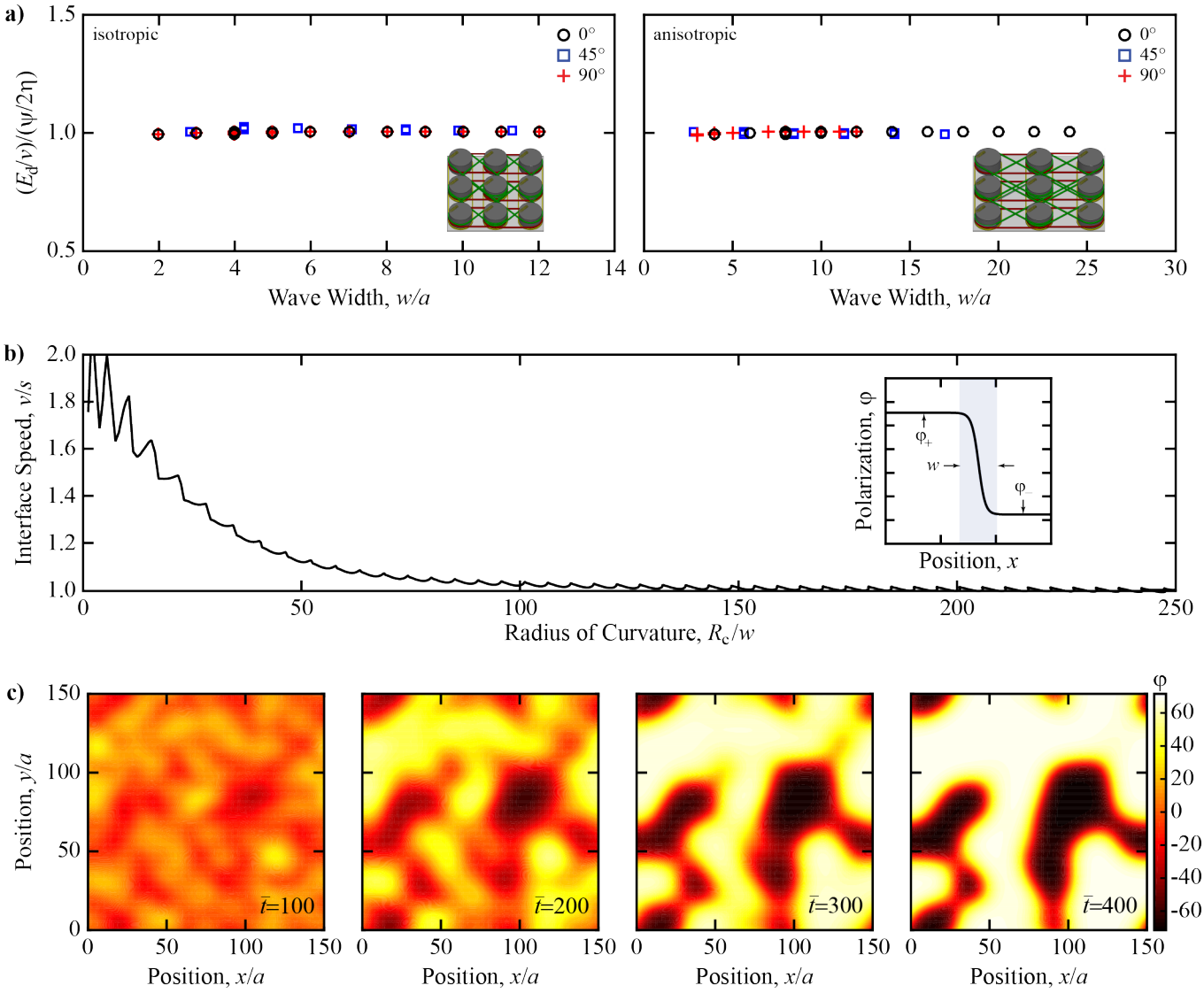

Figure 3. Domain wall motion obeys fundamental governing laws of energy transport and phase separation. a) Planar domain walls follow the kinetics of Equation (5). b) The measured speed of gently curved ($R_c \gg w$) domain walls resulting from phase separation are effectively predicted by the Allen-Cahn equation [29]. Inset: the profile of a transition wave interpolating the $\varphi-$ and φ_+ configurations with the approximated transition region (of width w) shaded. c) From noisy initial conditions, the mechanical system evolves homogeneous domains of either φ_- or φ_+ polarization, involving the motion of domain walls.

tia I. With the inertial and coupling conditions satisfied, the kinetics of phase separation within a system of oscillators is described by Equation (4). In particular, for smooth domain boundaries of sufficiently small curvature ς, the wall speed is predicted to be proportional to the local curvature, $v \sim \varsigma$ (the radius of curvature $R_c = 1/\varsigma$) [34]. Figure 3b compares the speed s of a propagating domain wall as obtained from the discrete system (Equation 2) and v from the Allen-Cahn model (Equation 4), with excellent agreement provided the curvature is small. Through a series of snapshots, Figure 3c illustrates the process of phase separation within a system of oscillators with periodic boundary conditions (see also Movie S2).

In summary, the reported purely elastic mechanical system displays several key features commonly found in atomic- or mesoscale physics of solids (thus mimicking atomic phenomena, or being *atomimetic*). The rotating-mass network shows qualitatively analogous features as, e.g., ferroic ceramics or phase-transforming solids, and the discrete governing equation was shown to approach the phase field equation commonly used to simulate the above processes, therefore demonstrating quantitative agreement if discreteness and inertial effects are sufficiently small (like in macroscale systems, entropic effects are not considered). This offers untapped opportunities for reproducing material-level, dissipative and diffusive kinetic phenomena at the structural level, which – in turn – invites experimental realization and paves the road to-

wards new active, intelligent, or phase-transforming mechanical metamaterials bringing small-scale processes to the macroscopically-observable scale.

METHODS

Material parameters of a lattice of bistable cylinders with nearest- and next-nearest-neighbor interactions – I, η, k_{ij}, and those within ψ – are rendered dimensionless as described in the Supplementary Information [29]. The governing equations of a $150a \times 150a$ system with periodic boundary conditions are numerically integrated via an explicit scheme [40]. The structure exhibits domain switching and phase transformation as described resulting in the formation and movement of domain walls whose kinetics are described by a scaling law and the Allen-Cahn equation. To verify the scaling law, we tilt the system by α such that the energy landscape remains double-welled but energetically favorable to one polarization (here φ_+). Initially of homogeneous φ_-, a line of sites is gradually rotated into φ_+, ultimately provoking the propagation of transition waves in the perpendicular direction. Here, the system has periodic boundary condition applied only along the propagating direction. The dimensions of the system are modified to allow domain walls sufficient time and space to achieve a steady state. Finally, to verify that the Allen-Cahn model describes the evolution of domain walls in the limit $|I\ddot{\varphi}| \ll |\eta\dot{\varphi}|$, we initialize the system with a circular domain (radius, $R_c = 55a$) of polarization φ_- within an otherwise uniform field of polarization φ_+ and monitor the speed s of the domain boundary (defined by $\varphi = 0°$).

SUPPORTING INFORMATION

Supporting Information is available from the Wiley Online Library or from the author kochmann@caltech.edu.

ACKNOWLEDGEMENTS

The authors acknowledge the support from the National Science Foundation (NSF) through CAREER Award CMMI-1254424.

[1] C. Chu and R. D. James, "Analysis of microstructures in Cu-14.O%A1-3.9%Ni by energy minimization," *Journal de Physique IV (Proceedings)*, vol. 5, pp. 143–149, December 1995.
[2] F. Jona and G. Shirane, *Ferroelectric Crystals*. Oxford/London/New York/Paris: Pergamon Press, 1962.
[3] W. Zhang and K. Bhattacharya, "A computational model of ferroelectric domains. Part I: model formulation and domain switching," *Acta Mater.*, vol. 53, no. 1, pp. 185–198, 2005.
[4] A. Onuki, *Phase Transition Dynamics*. Cambridge, UK: Cambridge Univ. Press, 2002.
[5] A. J. Bray, "Theory of phase-ordering kinetics," *Adv. Phys.*, vol. 51, no. 2, pp. 481–587, 2002.
[6] J. Christian and S. Mahajan, "Deformation twinning," *Prog. Mater. Sci.*, vol. 39, no. 1, pp. 1 – 157, 1995.
[7] J. M. Ball and R. D. James, *Fine Phase Mixtures as Minimizers of Energy*, pp. 647–686. Berlin, Heidelberg: Springer Berlin Heidelberg, 1989.
[8] D. Dye, "Shape memory alloys: Towards practical actuators," *Nat. Mater.*, vol. 14, pp. 760–761, 2015.
[9] C. S. Wojnar, J.-B. le Graverend, and D. M. Kochmann, "Broadband control of the viscoelasticity of ferroelectrics via domain switching," *Appl. Phys. Lett.*, vol. 105, no. 16, 2014.
[10] M. Fiebig, T. Lottermoser, D. Meier, and M. Trassin, "The evolution of multiferroics," *Nat. Rev. Mater.*, p. 16046, 2016.
[11] L. R. Meza, A. J. Zelhofer, N. Clarke, A. J. Mateos, D. M. Kochmann, and J. R. Greer, "Resilient 3d hierarchical architected metamaterials," *Proc. Natl. Acad. Sci.*, vol. 112, no. 37, pp. 11502–11507, 2015.
[12] T. Bueckmann, N. Stenger, M. Kadic, J. Kaschke, A. Froelich, T. Kennerknecht, C. Eberl, M. Thiel, and M. Wegener, "Tailored 3D Mechanical Metamaterials Made by Dip-in Direct-Laser-Writing Optical Lithography," *Adv. Mater.*, vol. 24, no. 20, pp. 2710–2714, 2012.
[13] H. Wadley, "Multifunctional periodic cellular metals," *Philos. Trans. R. Soc. A*, vol. 364, no. 1838, pp. 31–68, 2006.
[14] S. Krödel, T. Delpero, A. Bergamini, P. Ermanni, and D. M. Kochmann, "3D Auxetic Microlattices with Independently Controllable Acoustic Band Gaps and Quasi-Static Elastic Moduli," *Adv. Eng. Mater.*, vol. 16, no. 4, pp. 357–363, 2014.
[15] K. H. Matlack, A. Bauhofer, S. Krödel, A. Palermo, and C. Daraio, "Composite 3D-printed metastructures for low-frequency and broadband vibration absorption," *Proc. Natl. Acad. Sci.*, vol. 113, no. 30, pp. 8386–8390, 2016.
[16] L. R. Meza, S. Das, and J. R. Greer, "Strong, lightweight, and recoverable three-dimensional ceramic nanolattices," *Science*, vol. 345, no. 6202, pp. 1322–1326, 2014.
[17] Y. Chen and L. Wang, "Periodic co-continuous acoustic metamaterials with overlapping locally resonant and bragg band gaps," *Appl. Phys. Lett.*, vol. 105, no. 19, 2014.
[18] J. Paulose, A. S. Meeussen, and V. Vitelli, "Selective buckling via states of self-stress in topological metamaterials," *Proc. Natl. Acad. Sci.*, vol. 112, no. 25, pp. 7639–7644, 2015.
[19] D. Yang, L. Jin, R. V. Martinez, K. Bertoldi, G. M. Whitesides, and Z. Suo, "Phase-transforming and switchable metamaterials," *Extreme Mechanics Letters*, vol. 6, pp. 1 – 9, 2016.

[20] S. H. Kang, S. Shan, W. L. Noorduin, M. Khan, J. Aizenberg, and K. Bertoldi, "Buckling-induced reversible symmetry breaking and amplification of chirality using supported cellular structures," *Adv. Mater.*, vol. 25, no. 24, pp. 3380–3385, 2013.

[21] S. H. Kang, S. Shan, A. Košmrlj, W. L. Noorduin, S. Shian, J. C. Weaver, D. R. Clarke, and K. Bertoldi, "Complex ordered patterns in mechanical instability induced geometrically frustrated triangular cellular structures," *Phys. Rev. Lett.*, vol. 112, p. 098701, 2014.

[22] L. Landau, "On the theory of phase transitions (in russian)," *Zh. Eksp. Teor. Fiz.*, vol. 7, pp. 19–32, 1937.

[23] A. Devonshire, "XCVI. Theory of barium titanate," *Philos. Mag. Series 7*, vol. 40, no. 309, pp. 1040–1063, 1949.

[24] A. Devonshire, "CIX. Theory of barium titanate: Part II," *Philos. Mag. Series 7*, vol. 42, no. 333, pp. 1065–1079, 1951.

[25] N. Nadkarni, A. F. Arrieta, C. Chong, D. M. Kochmann, and C. Daraio, "Unidirectional transition waves in bistable lattices," *Phys. Rev. Lett.*, vol. 116, p. 244501, Jun 2016.

[26] J. Raney, N. Nadkarni, C. Daraio, D. Kochmann, J. Lewis, and K. Bertoldi, "Stable propagation of mechanical signals in soft media using stored elastic energy," *Proc. Natl. Acad. Sci.*, vol. 113, no. 35, pp. 9722–9727, 2016.

[27] N. Nadkarni, C. Daraio, and D. M. Kochmann, "Dynamics of periodic mechanical structures containing bistable elastic elements: From elastic to solitary wave propagation," *Phys. Rev. E*, vol. 90, p. 023204, Aug 2014.

[28] N. Nadkarni, C. Daraio, R. Abeyaratne, and D. M. Kochmann, "Universal energy transport law for dissipative and diffusive phase transitions," *Phys. Rev. B*, vol. 93, p. 104109, March 2016.

[29] M. Frazier and D. M. Kochmann, "Supplementary information," 2016.

[30] K.-C. Chen, W.-W. Wu, C.-N. Liao, L.-J. Chen, and K. N. Tu, "Observation of atomic diffusion at twin-modified grain boundaries in copper.," *Science*, vol. 321, pp. 1066–9, Aug. 2008.

[31] Y. Su and C. M. Landis, "Continuum thermodynamics of ferroelectric domain evolution: Theory, finite element implementation, and application to domain wall pinning," *J. Mech. Phys. Solids*, vol. 55, no. 2, pp. 280–305, 2007.

[32] J. Clayton and J. Knap, "A phase field model of deformation twinning: Nonlinear theory and numerical simulations," *Phys. D*, vol. 240, no. 910, pp. 841 – 858, 2011.

[33] S. Allen and J. Cahn, "Ground state structures in ordered binary alloys with second neighbor interactions," *Acta Metall.*, vol. 20, no. 3, pp. 423 – 433, 1972.

[34] S. M. Allen and J. W. Cahn, "A microscopic theory for antiphase boundary motion and its application to antiphase domain coarsening," *Acta Metall.*, vol. 27, pp. 1085–1095, June 1979.

[35] M. J. O'Neill, "The analysis of a temperature-controlled scanning calorimeter.," *Anal. Chem.*, vol. 36, no. 7, pp. 1238–1245, 1964.

[36] Approximately 0.5% of sites are selected as defective.

[37] P. Gao, J. Britson, J. R. Jokisaari, C. T. Nelson, S.-H. Baek, Y. Wang, C.-B. Eom, L.-Q. Chen, and X. Pan, "Atomic-scale mechanisms of ferroelastic domain-wall-mediated ferroelectric switching," *Nat. Commun.*, vol. 4, p. 2791, 2013.

[38] P. Gao, C. T. Nelson, J. R. Jokisaari, S.-H. Baek, C. W. Bark, Y. Zhang, E. Wang, D. G. Schlom, C.-B. Eom, and X. Pan, "Revealing the role of defects in ferroelectric switching with atomic resolution," *Nat. Commun.*, vol. 2, p. 591, 2011.

[39] We define the interface width as the space containing sites whose polarization deviates by more than 1% from either equilibrium state.

[40] G. Noh and K.-J. Bathe, "An explicit time integration scheme for the analysis of wave propagations," *Comput. Struct.*, vol. 129, pp. 178–193, August 2013.